



## Thermohydraulic performance of an array of microfluidic cells in unsteady non uniform heat loads distributions

Jérôme Barrau<sup>1</sup>, Luc Fréchette<sup>2</sup>, Joan Rosell<sup>1</sup>, Manel Ibañez<sup>1</sup>, Montse Vilarrubí<sup>1</sup>, Yina Bétancourt<sup>1</sup>, Gerard Laguna<sup>1</sup>, Ferran Badia<sup>1</sup>, Hassan Azarkish<sup>2</sup>, Louis-Michel Collin<sup>2</sup>

<sup>1</sup>University of Lleida, jerome.barrau@udl.cat, Lleida, Spain

<sup>2</sup>CRN2, Université de Sherbrooke, Sherbrooke, Canada

*jerome.barrau@udl.cat, Luc.Frechette@usherbrooke.ca, rosell@macs.udl.cat, m.ibanez@macs.udl.cat, mvilarrubi@macs.udl.cat, yinab@macs.udl.cat, gerard.laguna@udl.cat, fbadia@macs.udl.cat, Hassan.Azarkish@USherbrooke.ca, Louis-Michel.Collin@USherbrooke.ca*

**Abstract :** Within the high heat extraction cooling technologies, enhanced microchannels and hybrid jet impingement / microchannels cooling schemes are able to achieve relatively good temperature uniformities when submitted to steady state and uniform heat loads. Nevertheless, many applications, such as microelectronics, do not match these boundary conditions. In this work, the performance of a cooling scheme based on a matrix of microfluidic cells with individually variable coolant flow rate is numerically assessed under non uniform and unsteady heat load scenarios and compared with the ones of conventional microchannels. The results show that the pumping power needed by the cooling device to reach the temperature limitations of the cooled object are reduced by 30% with respect to conventional microchannels.

**Keywords :** Adaptive cooling, temperature uniformity, distributed cooling

### 1. Introduction

Many applications, such as electronics or solar concentration receivers, are submitted to increasing heat flux densities and need cooling devices that ensure their temperature control (safe function) without decreasing drastically their compactness. Liquid cooling devices based on microchannels [1] reach these goals as they provide very low thermal resistance coefficients. Nevertheless, this technology has two main drawbacks: One is their large pressure drop, that involves high pumping powers, and the other is the poor temperature uniformity of the cooled object, that implies reliability issues.

As a consequence, many papers and review articles are focused on enhanced microchannels [2-4] in order to deal with these inconvenients. Also other solutions, based on hybrid jet impingement /microchannel techniques have been proposed and tested experimentally [5-8]. Such cooling schemes have demonstrated their capacity to obtain prefixed temperature profiles along the coolant flow path (even uniform) when tailoring at the design stage their internal geometry to the heat loads. Furthermore, the hybrid jet impingement / microchannels devices generate less pressure losses than conventional microchannels and, as a consequence, need lower pumping powers [9,10].

However, these investigations are carried out through constant and uniform boundary conditions while heat load scenarios are, for example in electronic applications, usually unsteady and non-uniform. As a consequence, cooling devices with constant and uniform flow rate distributions are overly conservatives and lead to oversized pumping powers.

In this work, the thermo-hydraulic performance of a cooling device formed by a matrix of microfluidic cells with individually variable coolant flow rate is assessed under non-uniform and time dependent heat load scenarios.

## 2. Methodology

A matrix of microfluidic cells has been designed to both reduce the length of the coolant flow path, in order to reduce the pressure losses and to locally control the flow rate in each of the cell through self-regulated microvalves [11]. The aperture of these valves, located near the coolant outlet of each cell on the hot side of the cell (hottest point of the cooled object, in order to protect it from overheating), depends on their own temperature (Figure 1).

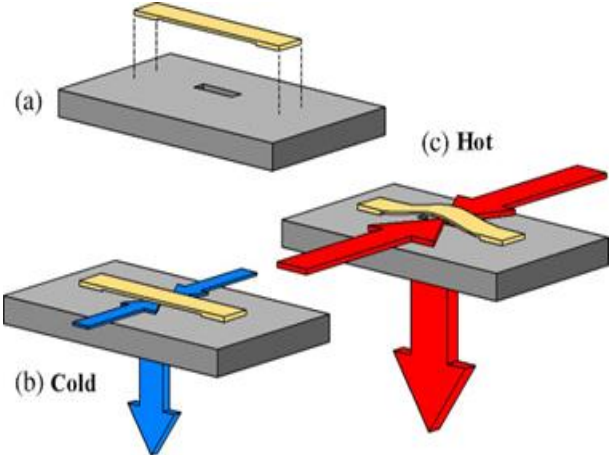
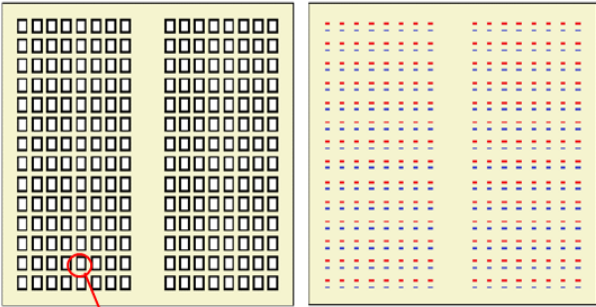


Figure 1 : Self adaptive microvalve (from [11])

### 2.1. Geometry

The cooling device is composed by several layers: the cooling layer, where the microfluidic cells are located, the slot layer, that represent the inlet and outlets of each of the cells, and the distribution layer, that ensure the coolant distribution from the inlet of the whole device up to its two outlets (Figure 2 and Figure 3).



One cell (see Figure 4, 5, 6)

Figure 2 : Arrangement of the matrix of microfluidic cells

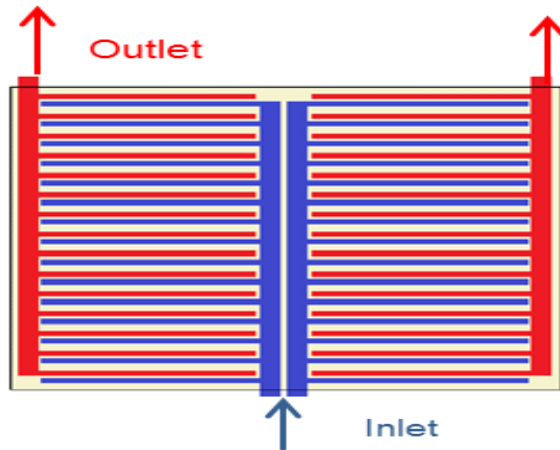


Figure 3 : Coolant distribution

Three internal geometries of the microfluidic cell are considered: without fins (MC0) (Figure 4), with fins (MC6) (Figure 5) and with tailored fins (MC6T) (Figure 6).

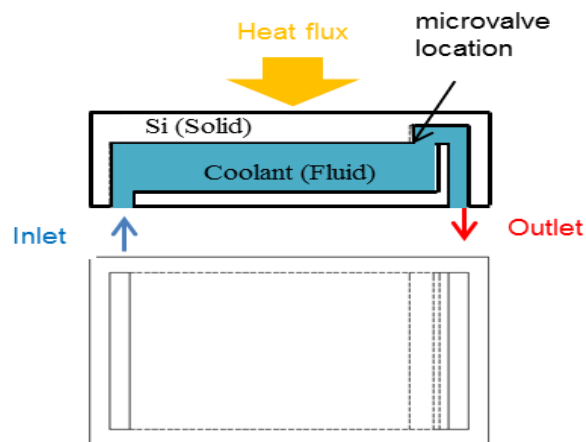


Figure 4 : Internal geometry of the microfluidic cell without fins (MC0)

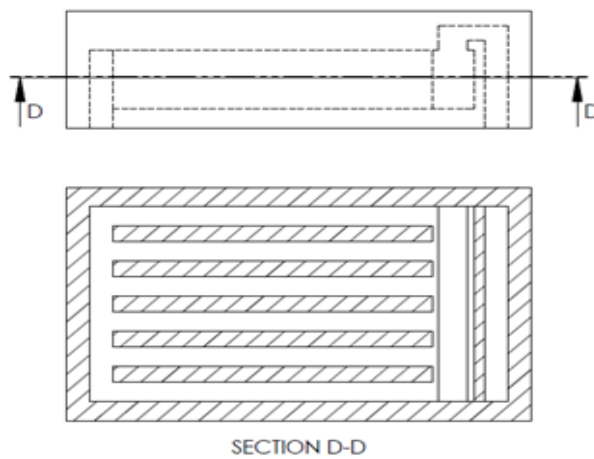


Figure 5 : Internal geometry of the microfluidic cell with fins (MC6)

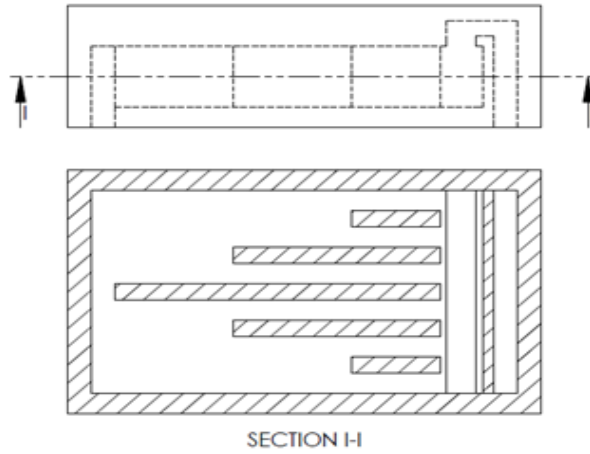


Figure 6 : Internal geometry of the microfluidic cell with tailored fins (MC6T)

The external dimensions of the cells are identical (Figure 7)

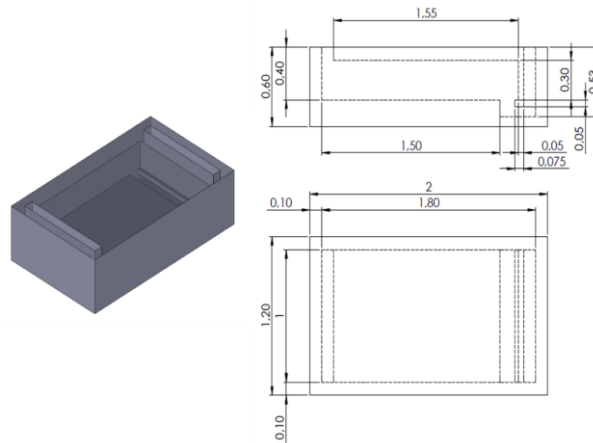


Figure 7 : MC0 design (dimensions in mm)

## 2.2. Numerical model

At a first stage, a numerical parametric study is carried out to assess the impact of the cells internal geometries on the pressure drop, the pumping power and the temperature uniformity while maintaining the maximum temperature of the cooled object below 100°C when submitted to the most demanding boundary conditions (heat flux: 300 W/cm<sup>2</sup>; inlet coolant temperature: 50°C).

For this steady-state study, the boundary conditions of the numerical models considered are as indicated in Figure 8.

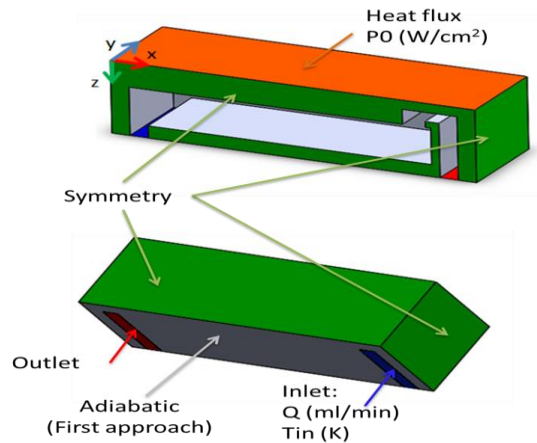


Figure 8 : Boundary conditions of the numerical model

The coupling between heat transfer and fluid flow is included in the COMSOL Multiphysics CFD model in a steady state study.

A laminar flow model has been chosen as the maximum Reynolds number is 6.

A mesh sensitivity analysis has been carried out and the final model accounts with 603921 elements.

### 2.3. Unsteady and non-uniform heat load scenario

At a second stage, a heat load scenario is defined and the performances along the time period considered is assessed (Figure 9 and Figure 10) and compared to the one of conventional microchannels.

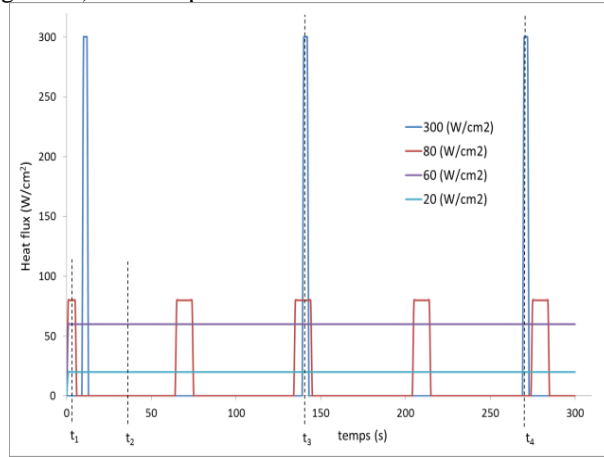


Figure 9 : Time dependence of the heat loads

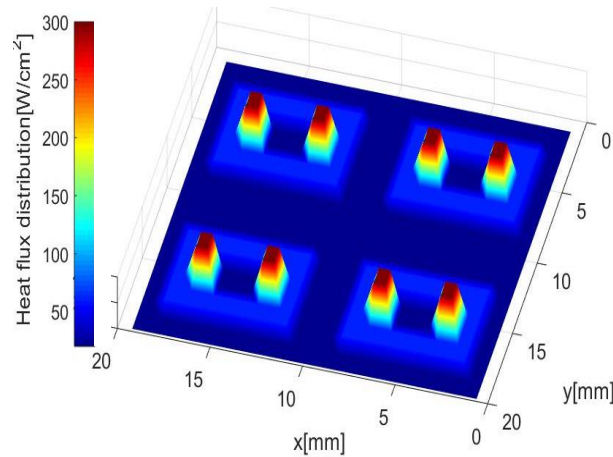


Figure 10 : Heat flux distribution at  $t_4$

In the steady state study, the maximum flow rate ( $Q_{max}$ ) needed to cool down the chip to its temperature limit is determined for each of the 3 proposed designs. In this unsteady analysis, these maximum flow rates are used as an input for the flow rate temperature dependences defined as follows:

$$Q(T) = Q_{max} * Q_{red} \quad (1)$$

where  $Q_{red}$  defines the opening of the valve and is defined according to Figure 11.

The valves start to open at a control value (80°C in Figure 11) and are totally opened at 10°C above the control value (90°C in Figure 11). Below the control value (80°C), a residual flow rate (1% of  $Q_{max}$ ) enters the cooling cell, since this kind of microvalve can't close completely. This general trend of valve function corresponds to the results obtained previously [11].

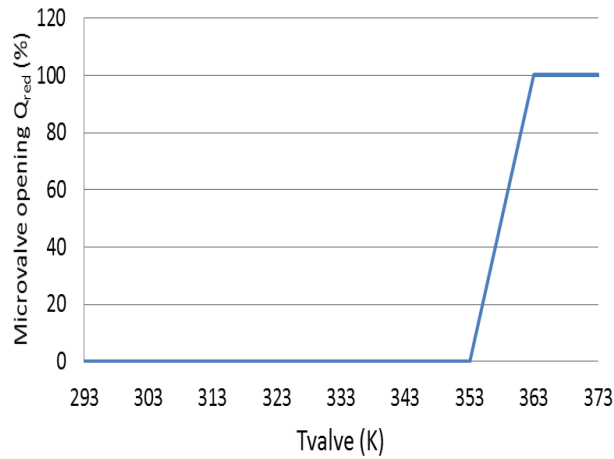


Figure 11 : Opening of the microvalve

For each of the 3 cell designs and for the conventional microchannels, a spatial integration of steady state results has been used to determine the temperature distribution obtained in the 4 heat load scenarios that occur during the time period.

### 3. Results and discussion

#### 3.1. Steady state study

The internal geometry with tailored fins (MC6T) shows a large improvement of the temperature uniformity with respect to other designs (Figure 12).

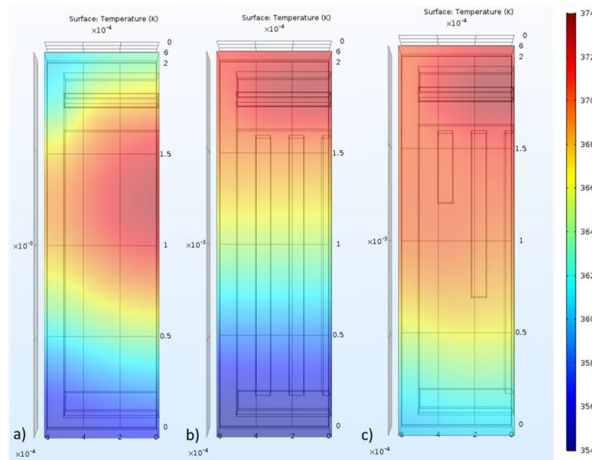


Figure 12 : Thermal map of the chip surface for a) MC0, b) MC6, c) MC6T heat flux:  $300 \text{ W/cm}^2$ ; inlet coolant temperature:  $50^\circ\text{C}$

The thermo-hydraulic performance of the 3 models of microfluidic cells is showed in Table 1, when submitted to the worst boundary conditions (Heat flux of  $300 \text{ W/cm}^2$  and inlet temperature of  $50^\circ\text{C}$ ). The flow rate was varied until the chip temperature was near  $100^\circ\text{C}$  ( $373\text{K}$ ).

Table 1 : Microfluidic cell steady state results

Model	Heat Flux ( $\text{W/cm}^2$ )	$T_{\text{in}}$ (K)	$Q_{\text{cell}}$ (ml/min)	R ( $\text{m}^2 \cdot \text{K/W}$ )	$\Delta P$ (Pa)	$\Delta T$ (K)
MC0	300	323.15	6.60	$1.41 \cdot 10^{-5}$	2728	17.6
MC6	300	323.15	2.64	$1.36 \cdot 10^{-5}$	834	19.2
MC6T	300	323.15	2.76	$1.50 \cdot 10^{-5}$	756	13.3

While the energetic performances of MC6 and MC6T designs are not substantially different (similar flow rate and pressure drops), the main advantage of the MC6T configuration is a better chip temperature uniformity

than the other two designs. Chip temperature differences are reduced (30%) from 19.2 K in MC6 to 13.3 K in MC6T.

**3.2. Unsteady and non-uniform heat loads**

*3.2.1. Flow rate*

In the case of microchannels, the flow rate can't be tailored to the time dependent heat flux distribution. As a consequence, the flow rate is constant in time and corresponds to the flow rate needed to meet the worst conditions, so highest heat rate while respecting the temperature limit (Figure 13).

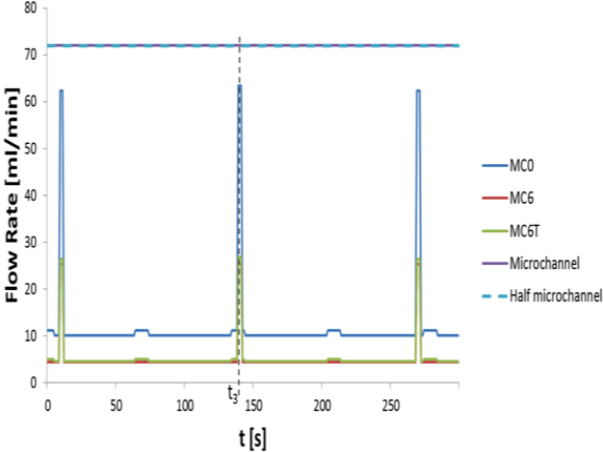


Figure 13 : Total flow rate along the time period

The total flow rate of the cooling device is, for all the heat load combinations, lower for the microfluidic cells than for the conventional microchannels. Also MC6 and MC6T need less flow rate than MC0 to reach the temperature limit as a consequence of their higher heat transfer capacity. The average flow rate, along the time period, of MC0, MC6 and MC6T represent, respectively 16.4%, 6.9% and 7.3% of the flow rates required with conventional microchannels (half-length and entire length).

*3.2.2. Pressure losses*

The maximum pressure drops of the microfluidic cooling devices and the conventional microchannels models are represented in Figure 14.

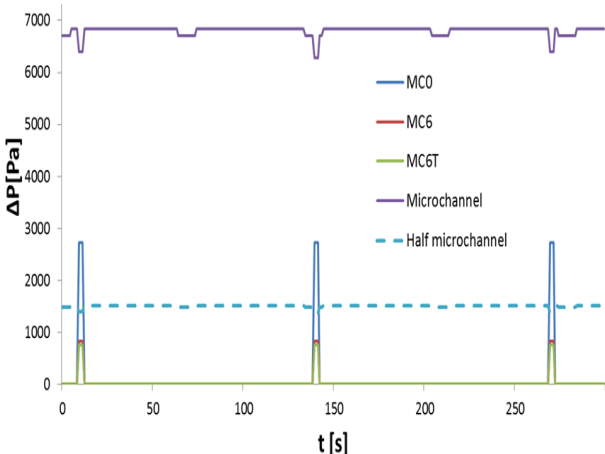


Figure 14 : Pressure drop along the time period

Assuming that the pump provides a constant pressure over time (conservative assumption), based on the cell with maximum pressure drop, we find that the required pressure for MC0, MC6 and MC6T are respectively 180%, 55% and 50% of the pressure drop in conventional microchannels (half-length). So low pressure losses can be achieved when appropriate fin designs are applied.

### 3.2.3. Pumping power

The assessment of the time dependents total flow rate and pressure drops provides the hydraulic pumping power trend along the time period considered (Figure 15).

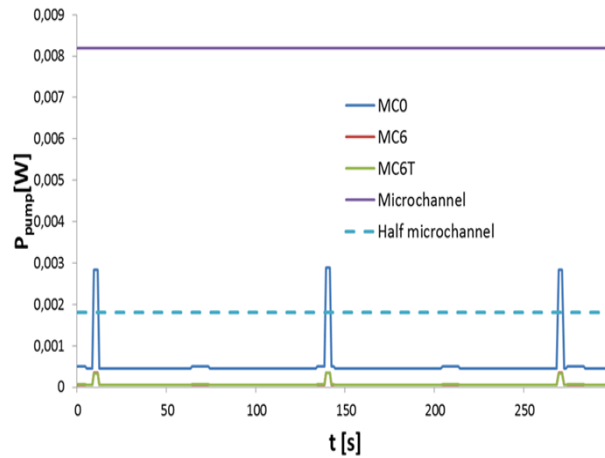


Figure 15 : Pumping power of the whole cooling device along the time period

For a similar performance (Temperature limitation) in comparable boundary conditions, the pumping energy needed, along the time period, by the matrix of microfluidic cells is shown to be between 4 and 30% the conventional microchannels one (half length).

### 3.3. Impact of the valve aperture function

The impact of the control temperatures at which the valve starts to open is studied, by varying it from 60°C to 90°C. The pumping energy ( $E_{Pump}$ ), assessed integrating the pumping power over the 5 minutes of the time period considered, corresponds to the worst boundary conditions defined by an inlet temperature of the coolant of 50 °C (Figure 16).

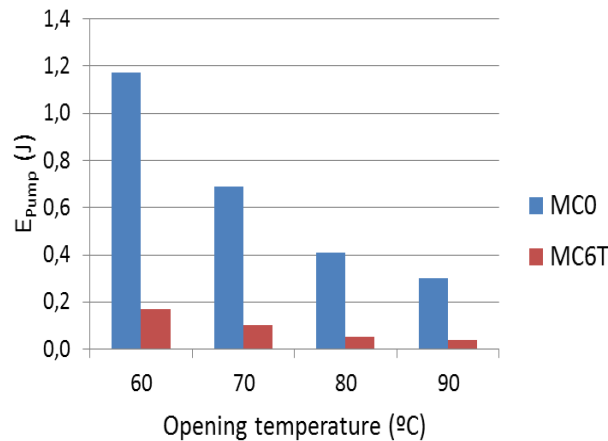


Figure 16 : Valve opening temperature sensitivity for MC0 and MC6T configurations

The results show that an increase in microvalve opening temperature always benefits the overall performance due to a flow rate reduction in those cells where thermal power dissipated allows microvalve to be partially opened or closed (residual flow rate).

## Conclusion

A cooling scheme based on a matrix of microfluidic cells with individually variable coolant flow rate is proposed with the aim of reducing the pumping energy consumption. Three internal geometries of the microfluidic cell are considered: without fins (MC0) with fins (MC6) and with tailored fins (MC6T). In the worst boundary conditions, the steady state study shows the tailored fins microfluidic cell has the best performance in terms of pressure drop and temperature uniformity. When integrating along a non-uniform and time dependent hat load distribution, the matrix of microfluidic cells achieve a pumping energy saving of 30% for the tailored fins design with respect to conventional microchannels. These results are the consequence of the two main characteristics of the cooling scheme: (1), the reduction of the pressure drop by 50% with respect to conventional microchannels, due to the short length of the coolant flow path and (2), the fact that the coolant flow rate of each cell is tailored to the local and time dependent heat extraction needs.

## Nomenclature

T	temperature, $K$	P	power, $W$
Q	flow, $ml.min^{-1}$	$\Delta P$	pressure, $Pa$
R	thermal resistance, $m^2.K.W^{-1}$	$E_{pump}$	pumping energy, $J$

## References

- [1] D.B. Tuckerman, F.W. Pease, *High-performance heat sinking for VLSI*, Electron Device Lett. IEEE, Volume 2, Pages 126-129, 1981.
- [2] P. Naphon, S. Wiriyasart, S. Wongwiset, *Thermal cooling enhancement techniques for electronic components*. International Communications in Heat and Mass Transfer, Volume 61, Pages 140-145, 2015.
- [3] M.G. Khan, A. Fartaj, *A review on microchannel heat exchangers and potential applications*, International Journal of Energy Research, Volume 35, Pages 553-582, 2011.
- [4] E.M. Dede, Y. Liu, *Experimental and numerical investigation of a multi-pass branching microchannel heat sink*, Applied Thermal Engineering, Volume 55, Pages 51-60, 2013.
- [5] S. Riera, J. Barrau, M. Omri, L.G. Fréchet, J. Rosell, *Stepwise varying width microchannel cooling device for uniform wall temperature: experimental and numerical study*, Applied Thermal Engineering, Volume 78, Pages 30-38, 2015.
- [6] J. Barrau, D. Chemisana, J. Rosell, L. Tadrist, M. Ibañez, *An experimental study of a new hybrid jet impingement/micro-channel cooling scheme*, Applied Thermal Engineering, Volume 30, Pages 2058-2066, 2010.
- [7] J. Barrau, M. Omri, D. Chemisana, J. Rosell, M. Ibañez, L. Tadrist, *Numerical study of a hybrid jet impingement/micro-channel cooling scheme*, Applied Thermal Engineering, Volume 33-34, Pages 237-245, 2012.
- [8] M.K. Sung, I. Mudawar, *Experimental and numerical investigation of single-phase heat transfer using a hybrid jet-impingement/micro-channel cooling scheme*, International Journal of Heat and Mass Transfer, Volume 49, Pages 682-694, 2006.
- [9] J. Barrau, J. Rosell, D. Chemisana, L. Tadrist, M. Ibañez - Effect of a hybrid jet impingement/micro-channel cooling device on the performance of densely packed PV cells under high concentration, Volume 85, Pages 2655-2665, 2011.
- [10] J. Barrau, A. Perona, A. Dollet, J. Rosell, *Outdoor test of a hybrid jet impingement/micro-channel cooling device for densely packed concentrated photovoltaic cells*, Volume 107, Pages 113-121, 2014.
- [11] M. McCarthy, N. Tiliakos, V. Modi, L.G. Fréchet, *Temperature-regulated nonlinear microvalves for self-*

*adaptive MEMS cooling*. Journal of Microelectromechanical Systems, Volume 17, Pages 998–1009, 2008.

### **Acknowledgements**

The research leading to these results has been performed within the STREAMS project ([www.project-streams.eu](http://www.project-streams.eu)) and received funding from the European Community's Horizon 2020 program under Grant Agreement n° 688564.

**25-27 Octobre 2017**  
**Monastir - Tunisie**